

Mathematical Modeling of Red Blood Cells Squeezing through Micro-capillaries and the Effect of Malaria Infection

Priyank Gullipalli¹ and Sarit K. Das^{1,*}

¹Department of Mechanical Engineering, Indian Institute of Technology Madras, Chennai, India

ABSTRACT

Red Blood Cells (RBCs) when infected by Malaria Parasites have altogether a different set of structural, biochemical and biophysical properties. These changes have drastic effects on the flow of these oxygen carrying cells in our body. The change in the biophysical parameters like the stiffness of the membrane is obtained experimentally and is available in the literature. The motion of the RBCs has been observed under the infected conditions. The RBCs becoming spherocytic, develops finger-like structures on its membrane which are observed but could not be analyzed as measurement at such small scale is extremely difficult. Hence, a computational model to replicate such motion is very essential for knowing the biophysical phenomena at such small scale. To overcome this limitation, a model has been developed for RBCs in the present study to simulate their flow under different conditions with or without infection computationally. This model successfully predicts the phenomena occurring in the flow of the RBCs when infected by the malaria parasite along with basic flow of RBCs squeezing through micro-capillaries. Our model predicts experimental observations available in literature successfully in case of Malaria affected RBCs. This gives us the leverage to extend this model to other types of cells when infected by diseases like Sickle Cell Anemia. As mentioned, this would be of great help in knowing how the biophysical quantities like pressure, stresses, etc are varying locally around the membrane of the RBC for a change in parameters such as capillary dimension or degree of parasite infection.

1. INTRODUCTION

Blood is a multiphase fluid that is made of red blood cells (RBCs), white blood cells and plasma. RBCs constitute ~40–45% of the total blood volume. Under normal, healthy conditions, an RBC is a biconcave disk with 8- μm diameter and 2- μm thickness. RBCs will squeeze through tiny capillaries less than their own diameter because of their high deformability to deliver their payload of oxygen and pick up waste carbon dioxide—functions essential to life.

In small vessels, the red blood cells have the tendency to move towards the centerline of the capillaries at the cost of deforming itself as the velocity is maximum at the centerline. This leads to collection of all the cells near the centerline. This provides the wall of the capillaries a cell free liquid layer. The lateral migration arises due to the deformation of the red blood cells as pointed out by Bishop et al [1]. A rigid particle would try to migrate near the wall as its tendency to deform is extremely low. Therefore, an increment in the stiffness reduces the tendency of the RBC to deform and hence squeeze through the center of the micro-capillaries.

Plasmodium falciparum is a severe malaria parasite typically characterized by brain, spleen, liver, or kidney pathology. Around the world, malaria is the most significant parasitic disease of humans and claims the lives of more children worldwide than any other infectious disease. The severity of

*Correspondence: HTTP #203, Department of Mechanical Engineering, IIT Madras, Chennai - 600 036, skdas@iitm.ac.in

P. falciparum infection is a function of capillary blockage by infected cells in these organs. Normal erythrocytes are highly deformable liquid-filled compartments as stated by Eggleton and Popel [2]. They owe their high degree of deformability to low internal viscosity, high surface-area-to-volume ratio, and the highly elastic nature of the erythrocyte membrane and underlying cytoskeleton as observed in [1]. Particularly during the late stages of parasite development, infected erythrocyte become spherocytic, develops knob-like structures, and lose their native deformability. This loss of deformability is often cited as an important contributing factor in capillary blockage.

Significant progress has been made in the last few years in understanding the variation of the biophysical properties of the RBCs. The stiffness of the RBCs under different stages of malarial infection is available in the literature [3] which is obtained experimentally. Refractive Index maps of the RBCs under the three infected stages of malaria are shown in [4] depicting the variation in the size and shape of the infected RBC which is increasingly stiffer as the reproduction of malaria parasite grows. The variation in shape is due to the fact that these stiffer RBCs have been in blood moving through the body. The stiffness is measured under different stages of infection and different temperatures. It has been observed that the RBCs get stiffened with the attack of the parasite and this effect is magnified under high temperatures. But, it has been observed that malaria generally comes with high temperatures and the stiffness is even higher at these febrile temperatures. Hence, the stiffness values considered for the present simulation are those with infection and high temperature. The stiffness can be measured when the infected RBC is treated by a drug as done by Mills et al [3]. This gives us a measure of how well the drug is reacting to the infectious parasite attack.

The measurement of the given physical parameters was done by using a sophisticated technique comprising of Optical tweezers and bead mark on an RBC in [5]. As expected the measurement of all the biophysical, flow and biomechanical parameters is extremely difficult but is very essential for determining the behavior of the RBCs under different stages of infection and their response to the drugs. Hence, a computational work would be of great help as we can estimate the required values from the numerical simulation at hand. Many computational models were developed for modeling RBCs but the spring model suggested by Tsubota et al [6] is one of the better models among the models which modeled RBC membrane with a network of elastic members which has simulated the motion of the RBCs in a Poiseuille flow within the capillaries of size greater than that of the RBCs. But the phenomenon of RBCs squeezing through the capillaries of size less than the size of the RBCs hasn't been simulated successfully. Hence, simulating this along with the simulation of the motion of RBCs when affected by Malaria under such conditions would be a great help in predicting many local parameters which can bring important insight to the membrane failure process under infection. The important parameters that can be estimated include the stress profiles, pressure across the membrane, local velocities etc.

2. MATHEMATICAL MODEL

The RBC is modeled as a fluid droplet whose parameters are calculated from the other published parameters. However instead of treating a thin membrane separately, we have introduced an imposed value of interfacial tension (Surface tension). The stiffness in case of the normal RBC is analogous to the surface tension of the droplet in our model. Hence, our surface tension model has its values calculated based on its comparison with the spring model developed in [6]. The spring model assumes a spring network on the membrane of the RBC whose spring constants are measured and validated in the paper. This kind of model is assumed because RBC has a flexible membrane which can be modeled using springs with a certain amount of liquid inside the membrane.

In our approach, a hypothetical membrane is considered which initially an undistorted straight line. Now, we assume a hypothetical force deforming it into a curve whose equation is known to us.

The equation of the curve can be:

$$Y = -0.04X^2 + 0.4X \quad (1)$$

Fig. 1 shows a deformed membrane from a plane X-axis which was the membrane's initial position. Now from the spring model, we assume a fixed number of springs oriented as they are mentioned in [6].

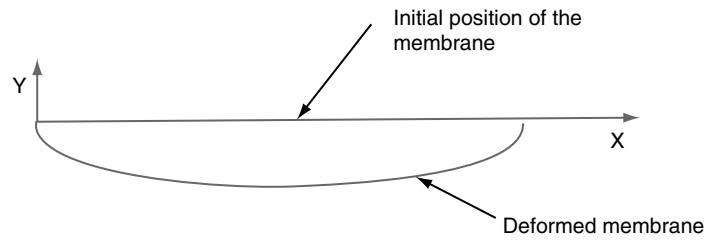


Figure 1. Initial and Final Positions of a membrane.

For the same deformation, the corresponding force equation is written in terms of the surface tension as the membrane now is considered as the free surface of the liquid.

The Surface Tension Model is formed as,

$$F = \int (\sigma/\kappa) dA \tag{2}$$

Where, σ = Surface Tension; κ = radius of curvature

Where, $dA = dl.l = (1 + (Y')^2)^{0.5}$ (3)

Now from the Spring Model;

$$F = K_l \sum \Delta X_l + K_b \sum \tan(\theta_l/2) \tag{4}$$

Where, X = the extension of the corresponding spring; θ = angle between two adjacent springs [9].

Equating the above two force equations, we get a relation between the surface tension (σ) and the spring constants (K_l, K_b) which is used to calculate the surface tension of the droplet. There are two different spring constants with different orientations where one is to take care of the linear extension; the other is to mimic the bending deformation of the membrane. The notion behind the presently developed model is to have a high-surface tension droplet to mimic the behavior of a membrane of the RBC.

The commercial CFD software FLUENT is used to model the two-dimensional, transient, two-phase Poiseuille flow in a micro-channel. We use the Volume of Fluid (VOF) method where we introduce the RBC as a droplet of diameter $6 \mu\text{m}$ as modeled in the literature [7] with other parameters either calculated or mentioned as in the literature.

2.1. VOF formulation

The volume-of-fluid method of [8] is used to identify the gas-liquid or liquid-liquid interface by solving a volume of fraction equation (Eq. 5) for the interface movement. An explicit geometric reconstruction scheme is used to represent the interface by using a piece-wise linear construction (PLIC) approach mentioned in [9]. The time step used for the VOF equation is not necessarily the same as that used for the other equations but is calculated based on the characteristic transit time of a fluid element across a control volume and is limited by a specific maximum value of the Courant number. The time taken to empty a cell is calculated by dividing the volume of each cell by the sum of the outgoing fluxes in the region near the fluid interface. The smallest such time is used as the characteristic time of transit for a fluid element across a control volume. The Courant number is defined by Eq. (6) below and the major equation for advection of volume fraction in given by Eqn. (5) below:

$$\frac{\partial \alpha}{\partial t} + V \cdot \nabla \alpha = 0 \tag{5}$$

Where V is the velocity vector, α is the volume fraction of one of the phases and the Courant number:

$$Co = \frac{\Delta t}{\Delta x / V_{fluid}} \quad (6)$$

Where Δx is the grid size and V_{fluid} is the fluid velocity. A maximum Courant number of 0.25 is set in the present calculations and a variable time-step based on a fixed Courant number of 0.25 or less was used to force the time step to be the same for all the equations.

2.2. Surface tension model

The continuum surface force (CSF) model proposed by Brackbill et al [10] is used to model surface tension effects. The CSF model approximates the surface tension-induced stress by a body force, which acts throughout a small but finite fluid region surrounding the interface.

The normal n and the curvature k in Eqn. (7) are defined in terms of the volume fraction (α) via:

$$n = \frac{\nabla \alpha}{|\nabla \alpha|} \quad (7)$$

And

$$\kappa = \nabla \cdot n \quad (8)$$

This implementation of the surface tension force can induce unphysical velocity near the interface known as the ‘spurious currents’ ([11], [12]). This occurs because the pressure and viscous force terms do not exactly balance the surface tension force. The accurate calculation of gradients can help minimizing the spurious currents.

2.3. Solution algorithm

An implicit body force treatment (for the surface tension force in the present case) is used to take into account the partial equilibrium of the pressure gradient and body forces. The present algorithm uses a co-located scheme in which pressure and velocity are stored at the cell centers to the cell faces. In the present computations, a body-force-weighted interpolation scheme is used to compute the face pressure by assuming the normal gradient of the difference between the pressure and body forces to be a constant.

A first order, non-iterative fractional step scheme is used for the time marching of the momentum and continuity equations. The correction tolerances for the sub-iterations (the ratio of the residuals at the current sub-iteration and the first sub-iteration) for pressure and momentum equations used are 0.01 and 0.001, respectively. The residual tolerance for both the equations was set to 0.0001. The specified values of correction tolerances are much lower than the default values of 0.25 for the pressure equation and 0.05 for the momentum equations.

The RBC is patched as a spherical bubble whose membrane should be finely demarcated instead of being blurred. Therefore, finer the grid better the membrane would be. Hence, a very fine grid of $0.2 \mu\text{m} \times 0.2 \mu\text{m}$ was chosen such that the results produced are independent of the grid spacing.

3. RESULTS AND DISCUSSIONS

Using the above model, we initially model the simple phenomenon of the RBCs squeezing through the micro-capillaries whose diameter is less than the size of the RBC. The thin layer of plasma formed between the deformed RBC and the wall of the capillary is successfully simulated in this model. The plasma is assumed to have a density of 1025 kg/m^3 with RBC having 1125 kg/m^3 and their viscosities being equal to and five times the viscosity of water.

Among the various capillary diameters and pressures given in [7], we choose the six diameters of 0.9, 1.4, 1.9, 2.2, 2.5 and 2.9 μm . Using the pressure range given in the paper for the particular diameters, we simulate the squeezing phenomenon. The validation (Fig. 2) of the simulations of RBCs squeezing through the capillaries of diameter less than that of the RBCs is carried out by comparing with the experimental results published in the paper. The comparison clearly indicates that the present simulation is able to replicate the features of RBC squeezing through the capillary.

The squeezing phenomenon is found to be successfully validated as shown in the Fig. 2. The figure illustrates the experimental results from [7] followed by the simulated results. The figure shows the mentioned set of diameters in the decreasing order from top to bottom and to the second column. The match can be found in terms of two of the important aspects that have to be looked into in this particular flow. The shape that the RBC has taken is parabolic which is in assent with our knowledge due to the velocity profile which is parabolic in a Poiseuille flow. The second aspect is to successfully simulate the micro-layer of plasma between the RBC and the wall of the capillary because this has not been simulated using the models established in the literature like the spring model by Tsubota et al [6]. This model has predicted this behavior as we have modeled it as a fluid and the squeezing of the RBC is nothing but a fluid trying to move into a constrained region by increasing its velocity. The problem with some of the solid models found in the literature (like the spring model by Tsubota et al [6]) is that this squeezing cannot assume a simple curvature and as the stress on the membrane is not uniform, this model would need more and more springs to predict the curvature better which might have held them back as they did not replicate the flow in micro-capillaries.

The model is then applied to simulate the effect of the malaria parasite on the flow of the RBCs in the micro-capillaries. The flow is observed under four different stages of infection and four different diameters accounting for the variation in the flow due to the parasite attack and the fluid Reynolds number.

The extension of the above model to the flow of RBC when affected by a malaria parasite also shows an excellent match (Fig. 3) with the experimental results published in [13]. It could depict the knob-like projections being formed on the surface of the RBC and more importantly the reduced affinity of

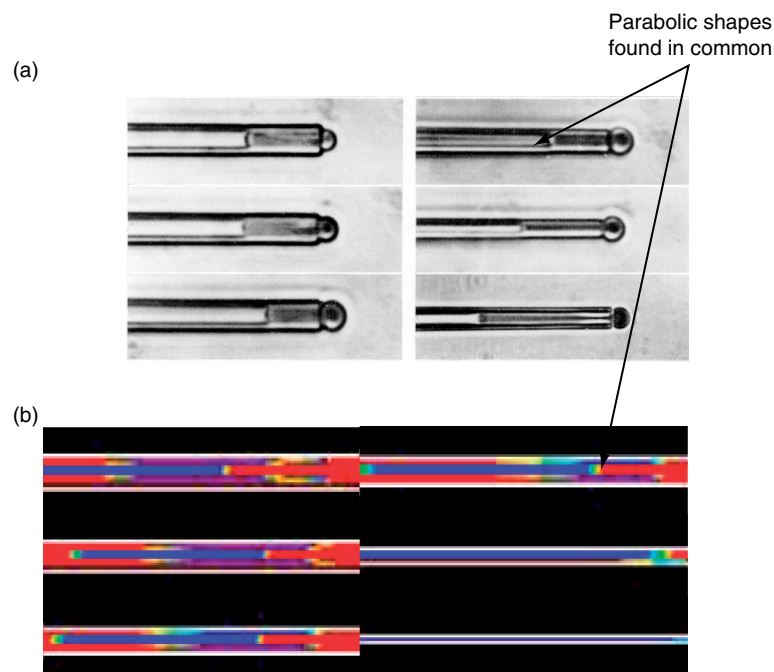


Figure 2. RBCs squeezing through the capillaries (a) Experimental (Ref [7]); (b) Computational.

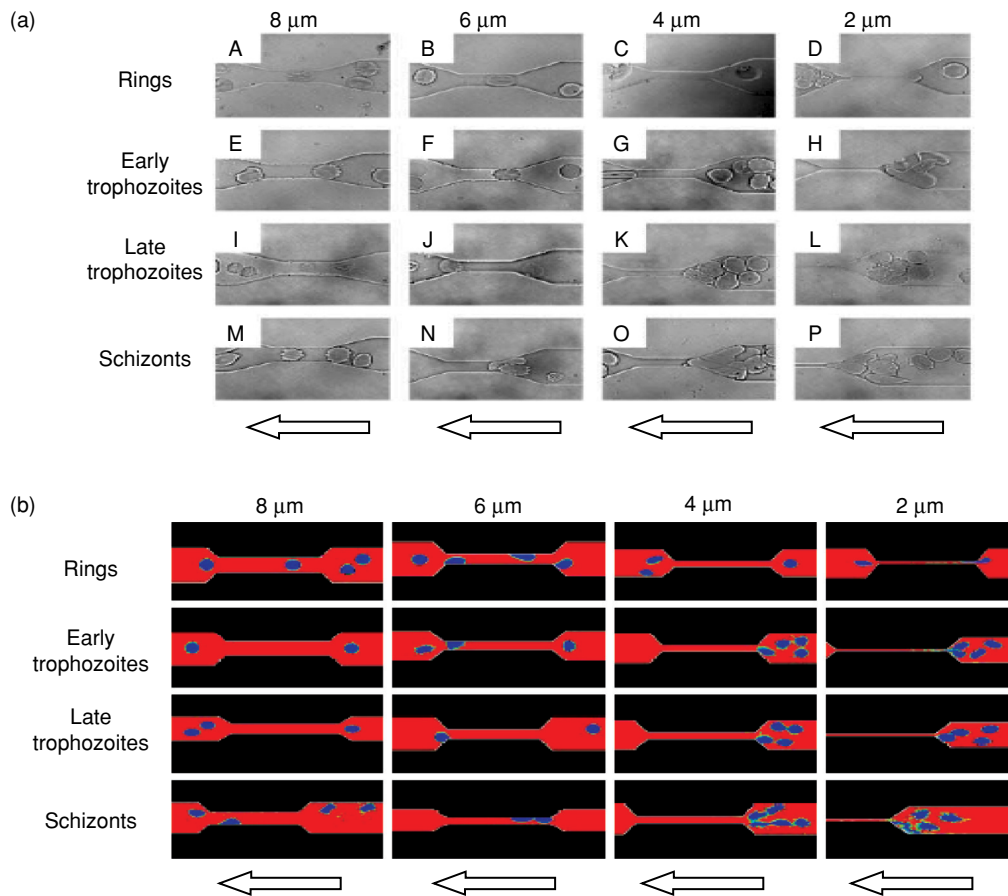


Figure 3. RBC flow when infected by Malaria under different flow conditions (a) Experimental (Ref [13]); (b) Computational.

the RBCs to squeeze through the lower capillary diameters at higher stage of infection. It has to be noted that the simulation result is extracted at the correct instant to make it possible to be comparable to the experimental results and that it is not the entire history of the flow of the RBC.

We have observed that the infected RBC movement is rather sluggish when compared to the flow of normal RBC movement as it nears the capillary. This leads to the occupation of more free flow area ahead of the capillary by a large number of RBCs which ultimately leads to the capillary blockage. In the Schizont stage of infection (the most infectious), the RBC near the 2 μm diameter doesn't readily try to get near to the capillary and is observed to ramble around instead of penetrating towards the capillary. This can be given a push by inducing it with an input flow velocity to move towards the capillary. Then it was observed to move sluggishly still showing no affinity towards penetrating and as the input velocity exceeds a certain value, the drop breaks into tiny droplets as it cannot take stress more than a specified value. Since the RBC fragmentation is unphysical, this limit in reality leads to rupture but the rupture mechanics are not included in our model. As pointed out earlier this might lead to more free space occupation and eventually lead to the blockage of the capillary. Sequestering of trophozoites and schizonts under capillary flow is an important mechanism by which the parasite avoids the spleen, where efficient mechanisms exist to destroy the parasite.

As the parasite reproduces, the biophysical characteristics of the cell change drastically leading to the increased infection whose stages are mentioned in the experimental results published in [13]. It can be observed from the simulated results (Fig. 3) that the RBC with the worst infection can penetrate through the 8 μm capillary (greater than the size of the RBC) as its size need not be altered here. As the infection grows, the Early and Late Trophozoite stages have difficulty in penetrating through 4 and

6 μm capillaries and cannot penetrate through the 2 μm capillary. The most infected Schizont can only penetrate through 8 μm capillary and to an extent into the 6 μm capillary. This is exactly replicated in our simulations providing an excellent replication.

A complete simulation of a couple of the cases is shown in Fig. 4 and Fig. 5. Fig. 4 is about how a healthy RBC successfully penetrates through a very thin 2 μm capillary in successive time steps without any problem. This is how the RBCs are expected to pass through the very small micro-capillaries delivering oxygen and collecting carbon-dioxide from the farther parts of the body from the heart. Fig. 5 shows the movement of a couple of infected RBCs in their most infected stage rambling around instead of penetrating into the capillary. It also shows the stiff knob-like shapes and projections on the membrane of the RBC. As this proceeds to happen more and more RBCs get clogged leading to the blockage (Fig. 6).

The variation of velocity with respect to the stiffness of the RBCs is plotted from the simulations for all the four diameters of the capillary as shown in Fig. 7. The velocity should decrease with the infection of the RBC. The pattern shown in the graph depicts the same pattern as expected. Since the tendency of the RBCs reduces to pierce through once the infection increases, they have lower velocities leading to blockage or sluggish movement through the capillaries. But, it can be observed from the graph that this trend has a certain slope for each of the capillary diameters and this effect is decreasing as the diameter increases. This evinces that as the RBCs have to squeeze more or as the need for deformation of the RBCs increase their velocity is affected more. The magnitude of velocity for the

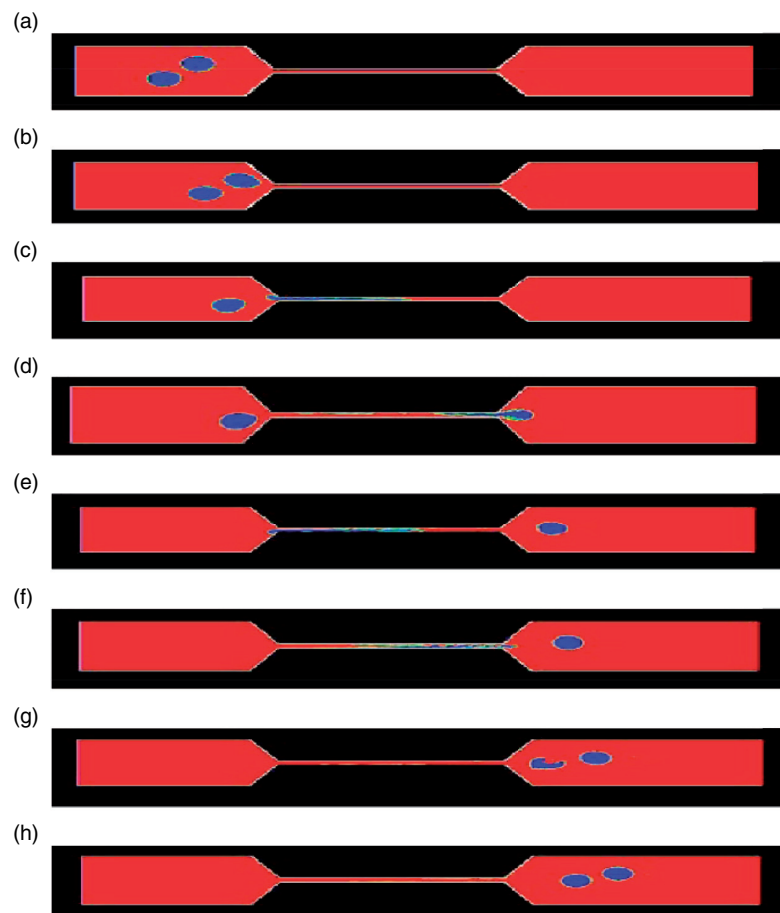


Figure 4. Healthy RBCs motion through a 2 μm capillary after (a) 10 time steps, (b) 40 time steps, (c) 60 time steps, (d) 90 time steps, (e) 120 time steps, (f) 150 time steps, (g) 180 time steps with a time step of 4×10^{-3} s.

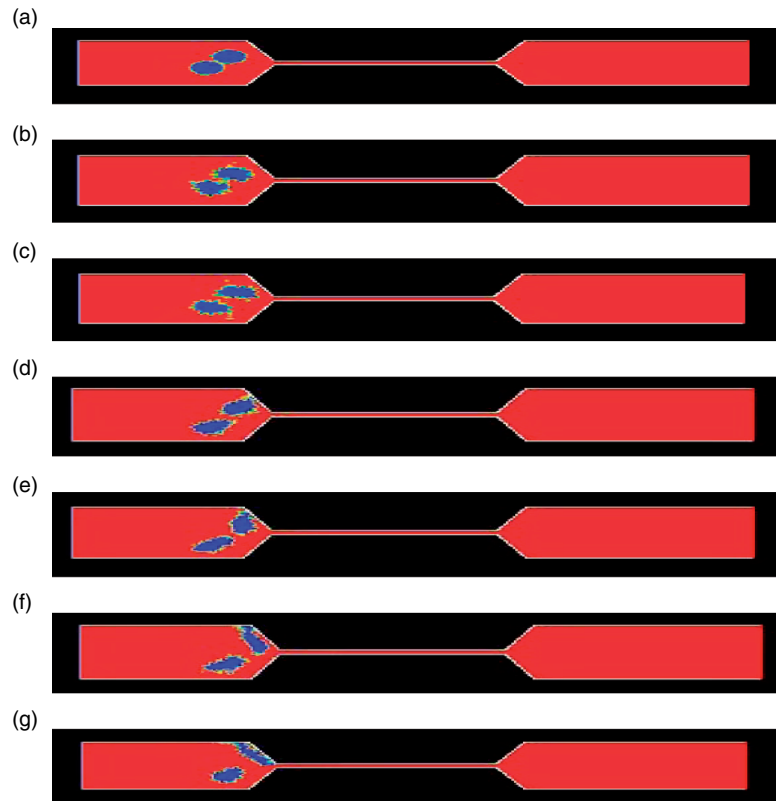


Figure 5. Schizont RBCs motion through a 2 μm capillary after (a) 8 time steps, (b) 16 time steps, (c) 20 time steps, (d) 24 time steps, (e) 28 time steps, (f) 32 time steps, (g) 36 time steps with a time step of 4×10^{-3} s.



Figure 6. Capillary Blockage enhanced with more number of Schizont RBCs crowding.

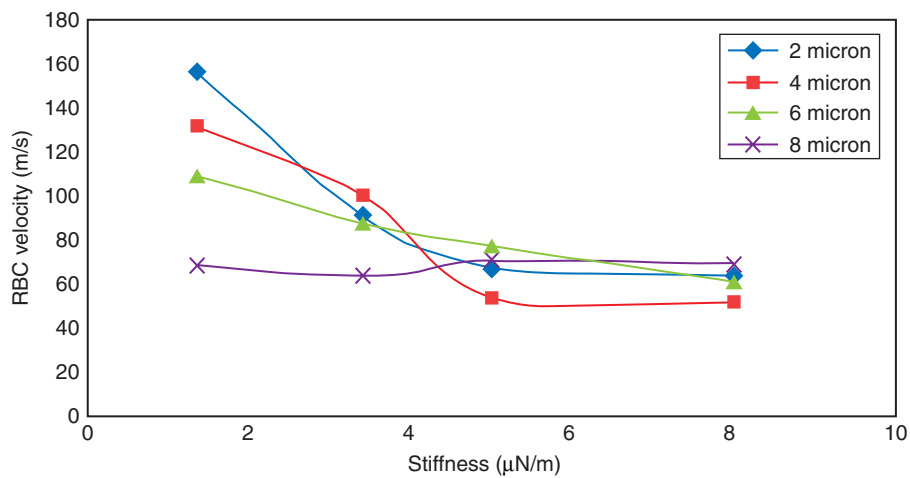


Figure 7. RBC velocity variations with the infection of the RBC.

healthy RBC is more in case of a 2 μm channel as it is expected from the continuity equation.

The RBC velocity variation is plotted as a function of the flow parameter, the fluid Reynolds number for all the four stages of infection in Fig. 8. The velocity of the RBCs must decrease with the decrease in the fluid Reynolds number as the Reynolds number is proportional to the velocity of the flow (which is the velocity the RBC is expected to have ideally). This effect can be clearly seen for a healthy (Ring Stage) RBC and this response is dampened as the infection increase. In the later stages of infection, the velocity of the RBC is less as it has fewer tendencies to penetrate through the micro-channel. Hence, its variation with the Reynolds number shown in the figure is negligible.

The model is subsequently applied to the case of sickle-cell anemia. Sickle-cell disease is a genetic life-long blood disorder characterized by red blood cells that assume an abnormal, rigid, sickle shape. Sickling decreases the cells' flexibility and results in a risk of various complications. The sickling occurs because of a mutation in the haemoglobin gene. Sickle-cell anemia can lead to various complications like *Stroke*, which can result from a progressive narrowing of blood vessels, preventing oxygen from reaching the brain. Cerebral infarction occurs in children and cerebral hemorrhage in adults.

In case of a malaria disease, the stiffness is increased in a malaria infected cell due to the multiplication of the malaria parasite within the RBC. But in sickle-cell disease, the process by which the stiffness increase is different. There is a mutation in the *HBB* gene in sickle cell disease, which encodes the beta-globin subunit of haemoglobin. The normal allele encodes a glutamate at position six of the beta-globin protein, whereas the sickle-cell allele encodes a valine. This change from a hydrophilic to a hydrophobic amino acid encourages binding between haemoglobin molecules, with polymerization of haemoglobin deforming red blood cells into a "sickle" shape. Such deformed cells are cleared rapidly from the blood, mainly in the spleen, for destruction and recycling.

Sickle Cell Anemia is another disease affected due to the increase in the stiffness of the RBC. The proposed model presented earlier is proved capable beyond any doubt to replicate complex squeezing phenomenon and the behavior of the malaria affected RBCs. The validation can clearly be cross-checked and can be found that this model is not only helping us to model complex phenomenon but also is predicting the same with a close proximity.

Hence, this phenomenon is extended to the flow of Sickle Cell Anemia under two different stress conditions. As predicted in [14], the Sickle Cell traverses faster than the healthy RBC under normal conditions and the opposite happens when a person undergoes a stressed situation. A person experiences normal pressure conditions when in normal state and the pressure increases towards the

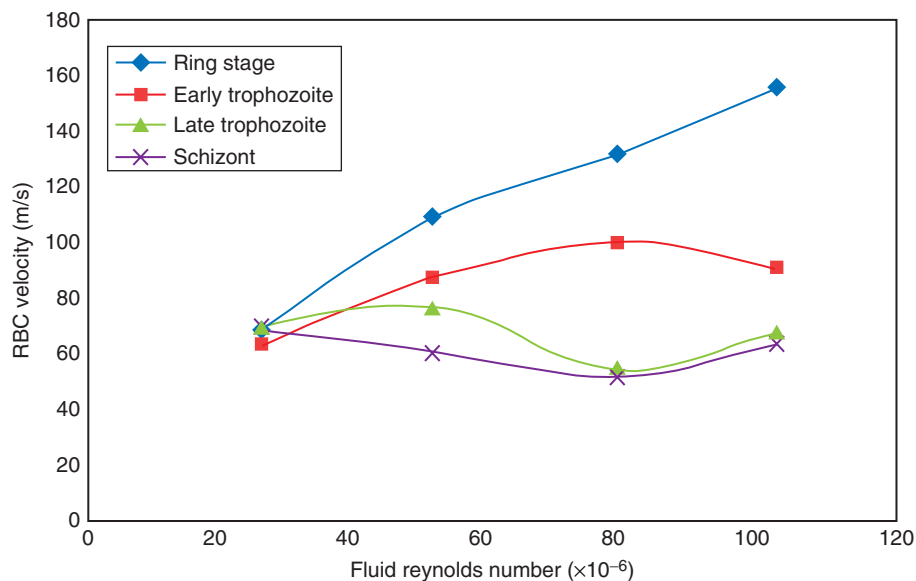


Figure 8. RBC velocity variations with the Fluid Reynolds number.

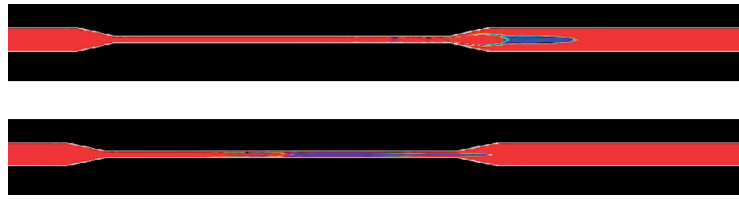


Figure 9. The state after 5000 time steps for (a) Sickle Cell, (b) Normal RBC with a time step of 4×10^{-6} .

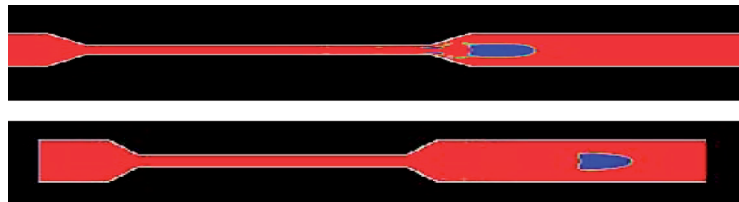


Figure 10. The state after 18000 time steps for (a) Sickle Cell, (b) Normal RBC with a time step of 2×10^{-6} .

farther ends of the body when he is in a stressful state.

The input and the output pressures are considered as mentioned in [15] along with the dimensions of the capillary which is $2.5 \mu\text{m}$ in diameter and the shear modulus of the Sickle Cell. The phenomenon observed was simulated successfully by the proposed model. Fig. 9 and Fig. 10 show the simulated results. These figures show the infected and the normal RBCs coming out of a constricted passage after a fixed time interval and it is found that both of them do not traverse with the same velocity. The RBC when infected travels faster under normal conditions (Fig. 9) but is the slower among the two in a stressful condition (Fig. 10).

4. CONCLUSION

A computational model has been developed to simulate the flow of the RBCs in constricted passages with specified flow conditions. This model successfully predicts the phenomenon occurring in the flow of the RBCs when infected by the malaria parasite along with basic flow of RBCs squeezing through micro-capillaries under normal condition. Since it is able to simulate complex phenomenon of finger-like projections forming on the membrane of the RBCs, their clogging of the capillaries, etc when the cells are infected with parasites, it gives us the leverage to extend this model to predict the flow behavior when infected by other diseases like Sickle Cell Anemia for which one of the observed basic phenomenon is simulated as a part of our work.

The versatility of using the simulations lie in the fact that it can consider coupled and decoupled effects of both parasite attack and temperature (which would change the numerical values in calculating the surface tension of the modeled droplet) to predict important parameters like pressure across the membrane, stress profiles and local velocities of the membrane helping the biologists to analyze the local cell behavior under specific parametric conditions. This would help the biologists to analyze the stress profiles across the membrane to examine the initiation of the rupture phenomenon which is of experimental interest. As stated before, this model helps them analyze the physical phenomenon in a relatively easier manner when compared to experimentation wherein obtaining the measurements at such micron level is tough, costly and time consuming.

This model also helps us to investigate the response of the cells to a particular drug (the parameters for which are available in literature) helping us to investigate the drug specific behavior under different possible scenarios mentioned. The strength in the model is to predict the flow accurately which makes the analysis easier when compared to what could have been done by experimentation as the velocity

patterns in each flow depicts the cell behavior as predicted.

REFERENCES

- [1] Bishop, J. J., A. S. Popel, M. Intaglietta, and P. C. Johnson. (2002) Effect of aggregation and shear rate on the dispersion of red blood cells flowing in venules. *Am. J. Physiol.* 283:H1985–H1996.
- [2] Eggleton, C.D., and A. S. Popel. (1998) Large deformation of red blood cell ghosts in a simple shear flow. *Phys. Fluids.* 10:1834–1845.
- [3] J. P. Mills, M. Diez-Silva, D. J. Quinn, M. Dao, M. J. Lang, K. W. S. Tan, C. T. Lim, G. Milon, P. H. David, O. Mercereau-Puijalon, S. Bonnefoy, and S. Suresh. (2007) Effect of plasmodial RESA protein on deformability of human red blood cells harboring *Plasmodium falciparum*. *PNAS.* 104(22):9213–9217.
- [4] YongKeun Park, Monica Diez-Silva, Gabriel Popescu, George Lykotrafitis, Wonshik Choi, Micheal S. Feld, and Subra Suresh. (2008) Refractive index maps and membrane dynamics of human red blood cells parasitized by *Plasmodium falciparum*. *PNAS.* 105(37):13730–13735.
- [5] Marina Puig-de-Morales-Marinkovic, Kevin T. Turner, James P. Butler, Jeffrey J. Fredberg, and Subra Suresh. (2007) Viscoelasticity of the human red blood cell. *Am. J. Physiol.* 293:597–605.
- [6] Ken-ichi Tsubota, Shigeo Wada, Takami Yamaguchi. (2006) Particle method for computer simulation of red blood cell flow. *Comp. Meth. prog. Biomed.* 83:139–146.
- [7] Alfred W. L. Jay. (1973) Viscoelastic properties of the human red blood cell membrane. *Biophysical J.* 13:1166–1182.
- [8] Hirt, C.W., Nichols, B.D. (1981) Volume of Fluid method for the dynamics of free boundaries. *J. Comp. Phy.* 39:201–225.
- [9] Youngs, D.L. (1982) Time-dependent multi-material flow with large fluid distortion. In: Morton, K.W., Baines, M.J. (Eds.), *Numerical Methods for Fluid Dynamics*. Academic, Newyork, pp. 273–285.
- [10] Brackbill, J.U., Kothe, D.B., Zemach, C. (1992) A continuum method for modeling surface tension. *J. Comp. Phy.* 100(2):335–354.
- [11] Lafaurie, B., Nardone, C., Scardovelli, R., Zaleski, S., Zanetti, G. (1994). Modelling, merging and fragmentation in multiphase flows with SURFER. *J. Comp Phy.* 113(1):134–147.
- [12] Harvie, D.J.E., Davidson, M.R., Rudman, M. (2006) An analysis of parasitic current generation in Volume of Fluid simulations. *App. Math. Mod.* 30(10):1056–1066.
- [13] J. Patrick Shelby, John White, Karthikeyan Ganesan, Pradipsinh K. Rathod, and Daniel T. Chiu. (2003) A microfluidic model for single-cell capillary obstruction by *Plasmodium falciparum*-infected erythrocytes. *PNAS.* 100(25):14618–14622.
- [14] S. A. Berger, B. E. Carlson. (2004) Sickle Cell Blood Flow in the Microcirculation. *IEEE.* 0-7803-8439-3/04:5057–5060.
- [15] M. M. Brandao, A. Fontes, M. L. Barjas-Castro, L. C. Barbosa, F. F. Costa, C. L. Cesar, S. T. O. Saad. (2002) Optical Tweezers for measuring red blood cell elasticity: application to the study of drug response in sickle cell disease. *Eur. J. Haematol.* 2003. 70:207–211.

